

Robust Liquid Container Transfer Control for Complete Sloshing Suppression

Ken'ichi Yano, *Associate Member, IEEE*, and Kazuhiko Terashima, *Member, IEEE*

Abstract—This paper is concerned with the advanced control of liquid container transfer, with special consideration given to the suppression of sloshing (liquid vibration) while maintaining a high speed of transfer for the container. In order to construct a high-speed transfer system for a liquid container that satisfies the reduction of endpoint residual vibration and has a robustness to change in the static liquid level, a suitable nominal model was adopted and an appropriate reference trajectory was determined by the optimization method of Fletcher and Reeves. Based on the above command inputs and using a suitable nominal model, an H^∞ feedback control system was applied to this process, and its effectiveness is shown through simulations and experiments. Furthermore, an active control method that takes into account the rotational motion of the container in addition to the linear transfer motion is presented, which can achieve complete suppression of sloshing during the whole transfer process.

Index Terms—Casting process, H^∞ control, liquid container transfer, manufacturing automation, optimization methods, robustness, sloshing.

I. INTRODUCTION

SLOSHING-SUPPRESSION problems have recently become of great importance in various fields. For example, the sloshing problem of liquid fuel inside the tanks of aerospace vehicles, the safety design of storage tanks for liquefied natural gas (LNG) and the design of water tanks to withstand earthquakes are significant areas of investigation. Also included in this field of study are liquid container transfer systems, such as those used for the transfer of molten metal from a furnace, motion control for automatic pouring in the casting and steel industries, as well as the transfer of perfume in perfume manufacture and beer in the alcohol industry, and so on.

In this paper, the control topics particularly focused on are liquid container transfer systems in the casting and steel industries. In practical industries such as these, it is essential to avoid excessive decreases in the temperature of the molten metal, as well as preventing any deterioration in quality due to contamination and to avoid overflow caused by sloshing. It is also important to shorten the total operational time in order to improve productivity. Therefore, it is necessary to construct a liquid container transfer system that will suppress sloshing as well as facilitate high-speed transfer.

Many studies have been published that deal with both the sloshing analysis in a container [1]–[6] and container transfer

with sloshing-suppression [7]–[20]. In [7] and [8], modeling and optimal control laws for several engineering specifications using linear quadratic integration (LQI) control for the transfer of rectangular containers were studied, with special consideration to the suppression of sloshing. In these studies, a simplex method was used in order to determine the optimum weighting matrix required to satisfy the respective specifications. The authors also present a computer simulation that was conducted using the boundary element method (BEM) in order to analyze the higher order sloshing modes [9], [10]. It was shown in this study that the first-mode sloshing was dominant in container transfer, and H^∞ control theory was applied to this transfer system in order to avoid spillover, as described in [10]. Sugie *et al.* studied a two-degree-of-freedom control structure in terms of stable factorization, where the feedforward part was constructed via a convex optimization and the feedback part was designed based on the H^∞ loop shaping method [11].

With respect to the shapes and transfer paths of the containers, historically, either narrow or three-dimensional rectangular containers that follow a straight path have been studied. By contrast, in more recent years the transfer of cylindrical-shaped containers and transfers involving a curved path have been of increasing interest. In [12] and [13], the optimum motion control system for an automotive, cart-based, cylindrical container was studied, with the main focus being on the suppression of sloshing on a curved transfer track. In [14], a methodology was given for the design of an optimal driving pattern for a moving cylindrical liquid container to reduce residual free-surface oscillations after a rapid access process. Furthermore, the optimum shape for such a container was studied by minimizing the performance index and considering both the resonant frequency of first-mode sloshing and the volume of liquid [15].

There are some studies that consider the robustness of the system. In [16], in order to enhance the robustness for the higher-mode sloshing, an algorithm was proposed for feedforward nonlinear optimal control over a specified frequency-range, and its application to the suppression of sloshing in linear container transfer was studied. In [17], the robustness of sloshing-suppression to changes in liquid level and viscosity using three-dimensional rectangular and cylindrical containers was analyzed in detail. It was pointed out that controlling this system by the conventional method of LQI control with a Kalman filter was considered to be difficult in the situation where the liquid level was lower than that described by the ratio of (liquid level)/(tank length) = 0.5.

Robustness to changes in the static liquid level, however, has not been yet guaranteed in any of the previous systems, although it was necessary to keep those systems stable with respect to

Manuscript received January 9, 1998. Manuscript received in final form January 17, 2001. Recommended by Associate Editor K. Wise.

The authors are with the Department of Production Systems Engineering, Toyohashi University of Technology, Aichi, Japan (e-mail: yano@procon.tutpse.tut.ac.jp; terasima@procon.tutpse.tut.ac.jp).

Publisher Item Identifier S 1063-6536(01)03366-8.

changes in liquid level after pouring and so on. Also, it was unable to prevent sloshing during the acceleration or deceleration phases of container transfer using only acceleration control, though residual vibration can be completely reduced at the endpoint, by which we mean the end time of the acceleration or the deceleration phase. This problem has to be solved in order to prevent deterioration in quality due to contamination and overflow. As regards this problem, Fukuda *et al.* [19] presented an active control system by using tank rotation for a narrow two-dimensional tank by using Housner model [1]. And Feddema *et al.* [20] also presented the system by using a robot arm. However, in their studies, the optimum control design did not pay sufficient attention to the problems of transfer time with sloshing suppression control and robustness to changes in liquid level.

Therefore, the purpose of this paper is to construct a liquid container transfer system that suppresses sloshing while transferring the container and which has robustness to changes in liquid level. Furthermore, a controller is found that allows the container to be transferred as fast as possible while meeting the specification for suppression of sloshing.

First, the sloshing characteristics of a rectangular container with respect to changes in liquid level is clarified, and a nominal model is constructed that minimizes the uncertainty range of the variation of model parameters with respect to changes in static liquid level.

Second, in order to achieve a high-speed transfer system as well as the required reduction of residual endpoint vibration, a reference trajectory was determined as a command input for the feedback control system using the optimization method of Fletcher and Reeves [21], combined with a clipping-off technique [22]. H^∞ control theory [23], [24] was applied to solve the robust control problem. Furthermore, a sloshing model was compiled comprising of two-degree-of-freedom including both of linear and rotational container motion, based on the concept of the pendulum-model. An active control method using additional rotational motion was introduced by H^∞ control in order to realize complete sloshing-suppression in the acceleration and deceleration phases of container transfer, as well as achieving the elimination of residual vibration at the endpoints.

Finally, the effectiveness of the control system applied in this paper is shown through simulations and experiments by comparing with conventional control methods, such as LQI control with a Kalman filter [8].

II. EXPERIMENTAL APPARATUS

A schematic diagram of an experimental apparatus is shown in Fig. 1. The size of the three-dimensional rectangular-type container is 0.14 [m] \times 0.14 [m] \times 0.3 [m] (length, width, height). A straight transfer path is used.

The container is moved using a dc servo-motor with a timing belt, and the velocity and position of the container are controlled by means of the voltage applied to the motor.

The position of the container is detected by a potentiometer fitted to a pulley. Displacement of the liquid level is detected through changes in resistance between the two stainless electrodes. The electrodes are installed 5×10^{-3} [m] from the side wall of the container. This position was used because the dis-

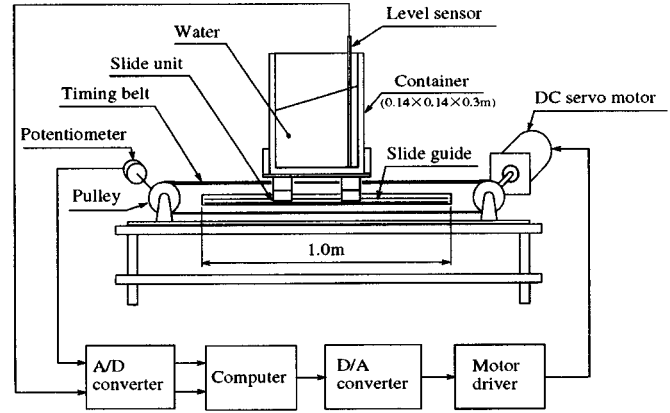


Fig. 1. Schematic diagram of experimental apparatus.

placement of the liquid level in the first-order mode sloshing can be observed near the side walls of the container, and because the sensor had to be slightly displaced from the side wall in order to avoid the effects of the wall.

Considering the similarity law in fluid dynamics, the object liquid in the experiment was water, because the Reynolds number of water at normal temperature is almost the same as that of molten iron metal or molten aluminum metal at high temperature. For example, the kinematic viscosities of iron molten metal at 1350 [K] and 1400 [K] are 1.365×10^{-6} [mPa \cdot s] and 1.237×10^{-6} [mPa \cdot s], respectively, while that of water is 1.0×10^{-6} [mPa \cdot s] at 293 [K]. Therefore, the fluid behavior of the molten metal may be fairly accurately predicted by the behavior of water. It enhances design safety if the control design is conducted using a fluid with lower damping characteristics, and for this reason we could use water as the target liquid in this study.

III. MODELING

A. Sloshing Model

Sloshing in a three-dimensional rectangular container can be approximated as a two-dimensional phenomenon as long as sudden changes in acceleration do not arise [8]. Therefore, in the present study, the sloshing phenomenon is described by a pendulum-type model [8]. The principles of this model are shown in Fig. 2, and by considering the moment balance around the fulcrum of a pendulum, the following equation is derived:

$$J \frac{d^2\theta}{dt^2} = -c \frac{d(\ell\theta)}{dt} \ell \cos^2\theta - mgl \sin\theta + m\alpha \ell \cos\theta \quad (1)$$

where

- J moment of inertia ($J = m\ell^2$);
- θ angle between the horizontal line and the liquid surface;
- α acceleration applied to the container.

This model contains an equivalent coefficient c of viscosity, considering both the viscosity of the liquid and the friction between the liquid and the wall. It also contains the mass m of liquid, the gravitational acceleration g and the equivalent length ℓ of the pendulum. The parameters ℓ and c of the above model were determined by experiments [8], where ℓ is also theoretically ob-

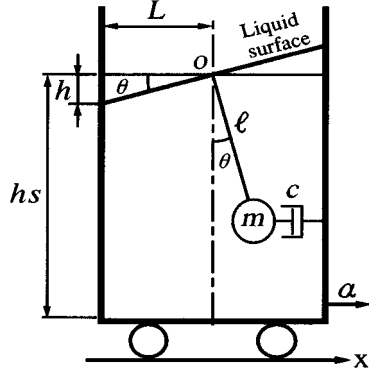


Fig. 2. Pendulum-type sloshing model.

tained based on the natural frequency determined by the perfect fluid theory [8]. The liquid level h at the right-side wall of the tank at the observation point L is represented by the equation $h = L \tan \theta$. Linearization of (1) gives

$$\ddot{\theta} = -\frac{c}{m}\dot{\theta} - \frac{g}{\ell}\theta + \frac{1}{\ell}\alpha. \quad (2)$$

B. System Model

For the dc servo-motor, the transfer function $G_m(s)$ from the input voltage $e(t)$ to the velocity $v(t)$ of the container is given as the following first-order lag model:

$$G_m(s) = \frac{V(s)}{E(s)} = \frac{K_m}{T_m s + 1} \quad (3)$$

where T_m is the time constant and K_m is the gain. These parameters were obtained by adding a step-wise input to the apparatus and then changing the output data from the position of the container to the velocity.

Using these parameters, linear vector state-space equations are obtained as follows, where the control input $e(t)$ is denoted as $u(t)$ and the position of the container as x . This model is controllable and observable

$$\dot{\mathbf{x}} = \mathbf{A}\mathbf{x} + \mathbf{B}u, \quad \mathbf{y} = \mathbf{C}\mathbf{x} \quad (4)$$

where

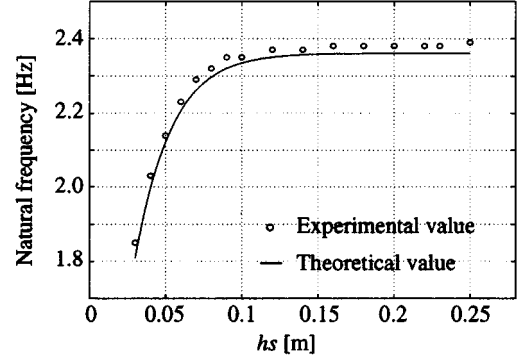
$$\mathbf{A} = \begin{bmatrix} 0 & 1 & 0 & 0 \\ -\frac{g}{\ell} & -\frac{c}{m} & 0 & -\frac{1}{\ell T_m} \\ 0 & 0 & 0 & 1 \\ 0 & 0 & 0 & -\frac{1}{T_m} \end{bmatrix}, \quad \mathbf{B} = \begin{bmatrix} 0 \\ \frac{K_m}{\ell T_m} \\ 0 \\ \frac{K_m}{T_m} \end{bmatrix} \quad (5)$$

$$\mathbf{C} = \begin{bmatrix} L & 0 & 0 & 0 \\ 0 & 0 & 1 & 0 \end{bmatrix} \quad (6)$$

$$\mathbf{x} = [\theta \quad \dot{\theta} \quad x \quad \dot{x}]^T, \quad \mathbf{y} = [h \quad x]^T.$$

IV. MODEL CHARACTERISTICS AND NOMINAL MODEL

In this section, the characteristics of the sloshing phenomenon for changes in liquid level are analyzed. Then the dominant natural frequency of the system is investigated, and the parameters,

Fig. 3. Relationship between liquid level h_s and natural frequency of sloshing.

c , m , ℓ , in (5) are obtained as the nominal model, where a nominal model is a model which is used in the control design. After this, the robust controller is designed.

The relationship between liquid level h_s and the natural frequency f_n is shown in Fig. 3. In general, the theoretical values of the natural frequency of sloshing is represented by (7), where ℓ_s is the length of the container and n is the dimension of the sloshing mode in (7).

$$f_n = \frac{\sqrt{g\kappa \tanh(\kappa h_s)}}{2\pi} \quad (7)$$

where

$$\kappa = \frac{(\pi n)}{\ell_s}, \quad n = 1, 2, \dots$$

These changes are associated with the depth of the liquid. The natural frequency of sloshing does not change at all when the liquid level is higher than 0.14 [m], as shown in Fig. 3. On the other hand, if the liquid level becomes lower than this fixed level, the natural frequency decreases. Therefore, controlling this system by the LQI control method [8] was considered to be difficult in cases with low liquid levels.

It is clear that the nominal model should not be selected for use at the middle point of the change in static liquid levels h_s , but instead at the middle point of the change in the natural frequency f_n . Therefore, the nominal model is determined in order to minimize the variation in the natural frequency of sloshing for the change in liquid level.

Assuming that the static liquid level changes from 0.03 [m] to 0.25 [m], the maximum value for the natural frequency obtained in the sinusoidal-wave shaking experiments is $f_n = 2.39$ [Hz] when $h_s = 0.25$ [m], and the minimum value of the natural frequency is $f_n = 1.85$ [Hz] when $h_s = 0.03$ [m], as seen in Fig. 3. Hence, the sloshing model with a natural frequency $f_{\text{nom}} = 2.12$ [Hz] is selected as the nominal model, where the nominal liquid level can be calculated by (7), and then $h_s = 0.0497$ [m], where $f_n = 2.12$ [Hz], $\ell_s = 0.14$ [m] and $n = 1$.

Then the parameter, m , in (5) is calculated, and c in (5) is obtained by the sinusoidal-wave shaking experiments. On the other hand, the natural frequency of (2) is represented by (8)

$$f = \frac{\sqrt{g/\ell}}{2\pi}. \quad (8)$$

TABLE I
NOMINAL PARAMETERS FOR THE SLOSHING MODEL

Parameter	Value	Unit
Length of pendulum, ℓ	0.055	m
Coefficient of viscosity, c	0.539	Ns/kg
Mass of liquid, m	0.975	kg
Nominal level, hs	0.0497	m
Motor gain, K_m	0.0913	m/sV
Time constant, T_m	0.0448	s

TABLE II
COMPARISON OF CONTROL SIMULATION RESULTS AT $hs = 0.03$

	Time	RV ($hs=0.03$ [m])	MA ($hs=0.03$ [m])
Case1	3.12[s]	1.04×10^{-2} [m]	1.42×10^{-2} [m]
		100.0[%]	100.0[%]
Case2	3.22[s]	2.19×10^{-3} [m]	9.70×10^{-3} [m]
		21.1[%]	68.4[%]
Case3	3.14[s]	4.58×10^{-3} [m]	1.06×10^{-2} [m]
		44.0[%]	74.6[%]
Case4	3.24[s]	3.22×10^{-3} [m]	1.04×10^{-2} [m]
		31.0[%]	73.2[%]
Case5	2.84[s]	5.43×10^{-4} [m]	7.90×10^{-3} [m]
		5.2[%]	55.6[%]

Case1 : Nominal level=0.14[m], LQI control, tentative trajectory

Case2 : Nominal level=0.0497[m], LQI control, tentative trajectory

Case3 : Nominal level=0.14[m], LQI control, optimal trajectory

Case4 : Nominal level=0.14[m], H^∞ control, tentative trajectory

Case5 : Nominal level=0.0497[m], H^∞ control, optimal trajectory

Therefore, the parameter, ℓ , in (5) is obtained by substituting $f = 2.12$ [Hz] in (8). Nominal parameters for the sloshing model are shown in Table I.

Simulation results designed by the conventional nominal liquid level ($hs = 0.14$ [m]) [8] and the proposed nominal level presented in this section are shown as Case1 and Case2, respectively, in the following tables. The cases where the liquid level $hs = 0.03$ [m] are shown in Table II and the cases of liquid level $hs = 0.14$ [m] are shown in Table III.

In the simulations, LQI control and a tentative reference trajectory are used, which is obtained by integrating the velocity curve that brings the tank into the target position at the limit of acceleration of the equipment. The time element is the transfer time for a 1 [m]-transfer of a container, RV is the maximum value of the residual vibration at the endpoint of the transfer, and MA is the maximum value of the sloshing amplitude caused in the acceleration and deceleration intervals. The amplitude ratios compared with Case1 in Table II are also shown in the tables, where the amplitudes in Case1 in Table II are set to 100[%].

From the results of simulations, good performance with respect to robustness to the reduction of the liquid level is realized by using the proposed nominal model. Therefore, it is considered that this present model is useful in order to achieve effective sloshing-suppression for changes in the liquid level. The reason why robustness was improved in this section of work will be explained by its connection with the control gains described in the following section. It is, however, unavoidable that this makes the transfer time longer, and also further excites sloshing in the

TABLE III
COMPARISON OF CONTROL SIMULATION RESULTS AT $hs = 0.14$

	Time	RV ($hs=0.14$ [m])	MA ($hs=0.14$ [m])
Case1	3.12[s]	1.87×10^{-4} [m]	1.31×10^{-2} [m]
		1.8[%]	92.3[%]
Case2	3.22[s]	1.25×10^{-3} [m]	8.15×10^{-3} [m]
		12.0[%]	57.4[%]
Case3	3.14[s]	1.37×10^{-4} [m]	8.70×10^{-3} [m]
		1.3[%]	61.3[%]
Case4	3.24[s]	6.97×10^{-4} [m]	8.80×10^{-3} [m]
		6.7[%]	62.0[%]
Case5	2.84[s]	4.20×10^{-4} [m]	7.50×10^{-3} [m]
		4.1[%]	52.8[%]

case where the liquid level is $hs = 0.14$ [m] and higher. Hence, in Sections V and VI, the reference trajectory and the control system are redesigned for the conventional method in Case1 [8] in order to construct a system that is much more robust.

V. OPTIMAL REFERENCE TRAJECTORY

In previous studies [8], a tentative reference trajectory that did not take into account sloshing-suppression was used as the command input. Therefore, in this study, in order to achieve a high-speed transfer system as well as the reduction of endpoint residual vibration, a reasonable reference trajectory for the feedback control systems was determined using the optimization method of Fletcher and Reeves [21], combined with a clipping-off technique [22].

An optimal trajectory was calculated in the following way. First, a terminal condition as shown in (9) is imposed to achieve both the target velocity (0.5 [m/s]) and the suppression of sloshing at the end-time of the acceleration. An optimal control problem that considers the restriction of the input magnitude of the actuator in the experimental transfer system can be formulated as (10), where the cost function J is formulated as a quadratic form in order to minimize the square norm of state error at the end-time of the acceleration interval, and where $t \in [t_o, t_f]$ is the interval of acceleration

$$\mathbf{x}_{t_f} = (\dot{x}, \theta, \dot{\theta})^T = (0.5, 0, 0)^T \quad (9)$$

$$\min_{\alpha} J = (\mathbf{x}_{t_f} - \mathbf{x}(t_f))^T \mathbf{W} (\mathbf{x}_{t_f} - \mathbf{x}(t_f))$$

subject to

$$\left. \begin{aligned} \frac{d}{dt} \begin{bmatrix} \dot{x} \\ \theta \\ \dot{\theta} \end{bmatrix} &= \begin{bmatrix} \alpha \\ \dot{\theta} \\ -\frac{c}{m}\dot{\theta} \cos \theta - \frac{g}{\ell} \sin \theta + \frac{1}{\ell} \alpha \cos \theta \end{bmatrix} \\ \mathbf{x}(t_o) &= (\dot{x}, \theta, \dot{\theta})^T = (0, 0, 0)^T \\ |\alpha| &\leq 2.0 \text{ [m/s}^2\text{]} \end{aligned} \right\} \quad (10)$$

Second, a nonlinear optimal theory based on the Fletcher and Reeves method, combined with a clipping-off technique is applied to solve the optimal control problem with constrained inputs. The interval of deceleration is known to be able to turn over the input of acceleration. Finally, an optimal reference trajectory is obtained by integration of the velocity curve for the total

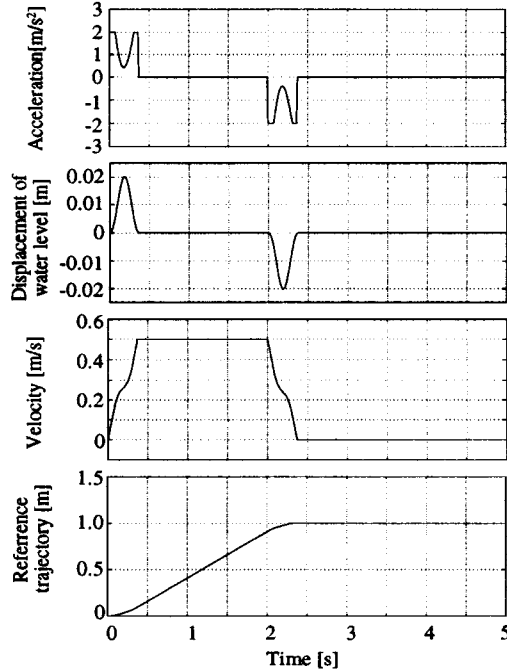


Fig. 4. Optimal reference trajectory.

interval. This method gives a minimum time for the acceleration interval of 0.37 [s], where $\mathbf{W} = \text{diag}[10^6, 10^6, 10^6]$. The optimal reference trajectory for the nominal model obtained in the previous section is shown in Fig. 4, but this trajectory is not a completely Bang-Bang-type input because the sampling time was set to 0.01 [s] for reasons of limitations in the hardware.

The effectiveness of this optimal reference trajectory is shown by comparing it with the results obtained by using the tentative reference trajectory in Case1. Through simulations and feedback control experiments, where the nominal liquid level was set to 0.14 [m] and LQI control was used for both cases, the influence caused by the reference trajectories alone was evaluated. In this case, the nominal model was set at 0.14 [m], and the minimum time of the acceleration interval was 0.34 [s]. The simulation results with the optimal reference trajectory are shown in Case3 in Tables II and III. Furthermore, experimental results of the tentative reference trajectory are shown in Fig. 5(a), and those for the optimal reference trajectory are shown in Fig. 5(b), where the time of the acceleration interval for the tentative reference trajectory is 0.25 [s].

From these results, the maximum amplitude is suppressed from 1.42×10^{-2} [m] (100%) to 1.06×10^{-2} [m] (74.6%) at the lowest liquid level ($hs = 0.03$ [m]), and from 1.31×10^{-2} [m] (92.3%) to 8.70×10^{-3} [m] (61.3%) at a nominal liquid level of ($hs = 0.14$ [m]), with almost the same transfer time. Furthermore, the residual vibration as well as the maximum amplitude is quite well suppressed for both cases where $hs = 0.03$ [m] or 0.14 [m]. As a result, the data for Case3 show better results compared with those for Case1 in all performances. Hence, the optimal reference trajectory that achieves a reduction in the end-point residual vibration as well as the maximum amplitude is obtained by using the optimization method of Fletcher and Reeves, combined with a clipping-off technique.

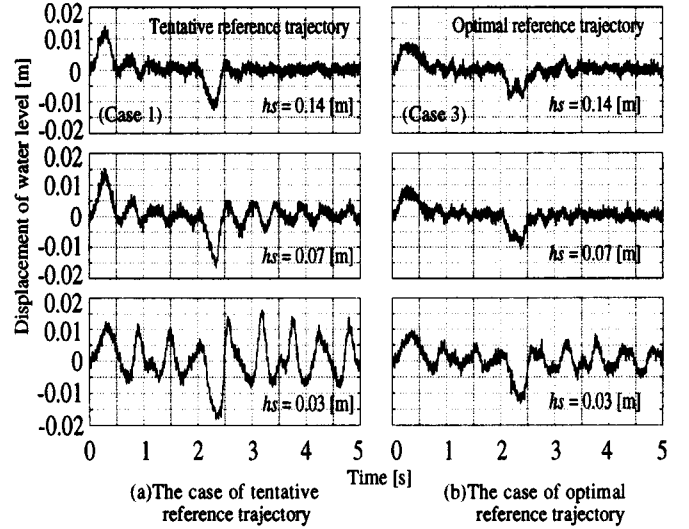
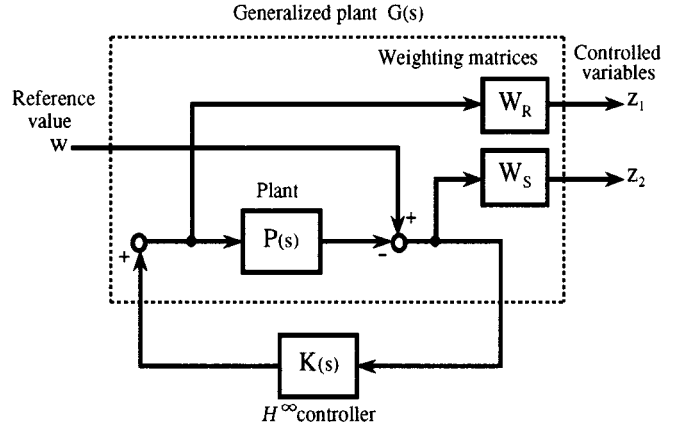


Fig. 5. Simulation results with a tentative reference trajectory (Case1) and an optimal reference trajectory (Case3).

Fig. 6. Augmented closed loop system for H^∞ control design.

VI. CONTROL SYSTEM DESIGN AND RESULTS

A. H^∞ Control

The H^∞ feedback control system is designed using the optimum reference trajectory and the proposed nominal model. An augmented closed-loop system is constructed as shown in Fig. 6. The H^∞ controller [23], [24] is designed to satisfy the following mixed sensitivity problem, as shown in (11):

$$\left\| \begin{matrix} W_S S \\ W_R R \end{matrix} \right\| < \gamma. \quad (11)$$

Since the mixed sensitivity problem considering the additive variations of model uncertainty is applied to this study, an uncertainty weight W_R and a sensitivity weight W_S are given.

Frequency responses of the transfer function to additive variations of model uncertainty against a nominal model are shown in Fig. 7. In order to enhance the robustness for this model uncertainties against changes in liquid level, spillover avoidance and noise rejection, the uncertainty weight W_R is given to be

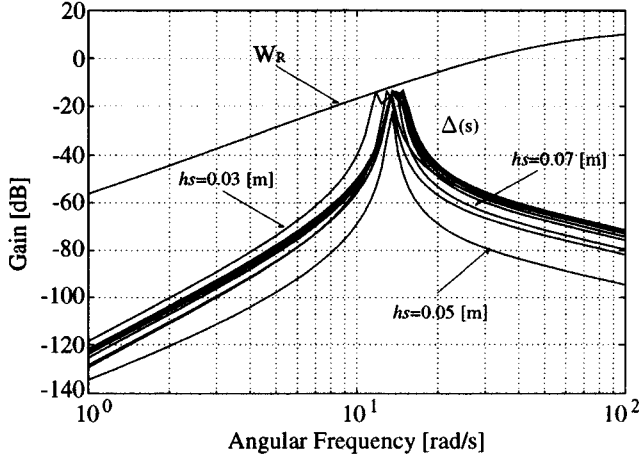


Fig. 7. Frequency responses of the additive uncertainties against the nominal model and its uncertainty weight.

monotonically increased, as shown in Fig. 7. Its value is shown in (12)

$$W_R = \frac{8.4 \times 10^{-2}(5s+1)(10s+1)}{(s+40)(s+70)}. \quad (12)$$

Next, the sensitivity weight W_S is considered. Each diagonal element of W_S is given as a different value, as shown in (13), because this system is a regulator system for the suppression of sloshing and also a servo-system for the position of the container. In particular, the weighting function for the position of container is set to be high gain, at around $\omega = 0$ in order that it can operate as a servo-system

$$W_S = \begin{bmatrix} \frac{\alpha_r}{s+1} & 0 \\ 0 & \frac{\alpha_s}{s+10^{-4}} \end{bmatrix}. \quad (13)$$

There is, however, a tradeoff between these two features, because the present system features one input but two outputs. So, in order to make a fair comparison with the LQI control, a servo gain α_s of W_S was given to yield faster transfer times than the LQI control theory. A regulator gain α_r will be given hereafter.

As a result, α_r and α_s were set to 7600 and 1650, respectively. An eighth-order controller is obtained, as shown in (14), where the optimum value of γ is 7.71×10^3 . A MATLAB Robust Control Toolbox was used in the present control design

$$K(s) = [K_{h-u}(s) \quad K_{x-u}(s)] \quad (14)$$

where we have (15) and (16), shown at the bottom of the page. Each parameter of the controller is shown in Table IV.

TABLE IV
PARAMETERS OF THE CONTROLLER

i	a_i	b_i	c_i
1	1.33×10^{-6}	1.09×10^{-4}	9.70×10
2	1.35×10^3	4.36×10^9	4.64×10^3
3	1.35×10^7	4.74×10^9	1.39×10^5
4	1.18×10^6	4.16×10^8	2.62×10^6
5	1.08×10^5	3.71×10^7	2.86×10^7
6	6.71×10^3	2.22×10^6	1.56×10^8
7	1.62×10^2	5.27×10^4	1.30×10^8
8	1.22	3.94×10^2	1.30×10^4

B. Analysis for the Designed System

In order to compare with the previous results [8] of the LQI control system in Case1, whose nominal liquid level is 0.14 [m] and whose reference trajectory is the tentative trajectory, simulation results of the H^∞ control system are shown in Case5 in Tables II and III whose nominal liquid level is 0.0497 [m] and whose reference trajectory is the optimum trajectory obtained in Section V. Further comparisons are shown in Fig. 8, where the liquid levels in the figure are (a), (b), (c) 0.14 [m], (d) 0.03 [m], (e) 0.07 [m], and (f) 0.25 [m]. The transportation distance is 1 [m] and the sampling time is 0.01 [s]. In these simulations, the trajectory of the LQI control appears to be faster than the trajectory of the H^∞ control at the middle of the transfer, but the transfer times are 3.12 [s] for the LQI control and 2.84 [s] for the H^∞ control, respectively. Furthermore, the example where the system was designed by H^∞ control theory under the same trajectory and nominal model as Case1 was shown in Case4 in Tables II and III to evaluate only the differences between the control methods.

As seen in Fig. 8, both the H^∞ control and the LQI control methods effectively suppress sloshing when the liquid level is 0.14 [m]. Also, both control methods suppress sloshing when the liquid level is higher than 0.14 [m]. This is because the sloshing characteristics hardly change compared to the conventional nominal model as shown in Fig. 3. However, as the liquid levels decrease, it becomes difficult for the LQI control to suppress sloshing when compared to the H^∞ control. The difference in robustness for each change in liquid level is clearly shown when $h_s = 0.03$ [m]. For example, the maximum amplitude is suppressed from 1.42×10^{-2} [m] (100%) to 7.90×10^{-3} [m] (55.6%) and the residual vibration is suppressed from 1.04×10^{-2} [m] (100) to 5.43×10^{-4} [m] (5.2%) with the faster transfer time.

The frequency responses of the controller in Case5, obtained by using the H^∞ control theory, are shown in Fig. 9, where

$$u = [K_{h-u}(s) \quad K_{x-u}(s)] \begin{bmatrix} h \\ x \end{bmatrix} \quad (15)$$

$$K_h(s) = \frac{a_8 s^7 + a_7 s^6 + a_6 s^5 + a_5 s^4 + a_4 s^3 + a_3 s^2 + a_2 s + a_1}{s^8 + c_8 s^7 + c_7 s^6 + c_6 s^5 + c_5 s^4 + c_4 s^3 + c_3 s^2 + c_2 s + c_1}$$

$$K_x(s) = \frac{b_8 s^7 + b_7 s^6 + b_6 s^5 + b_5 s^4 + b_4 s^3 + b_3 s^2 + b_2 s + b_1}{s^8 + c_8 s^7 + c_7 s^6 + c_6 s^5 + c_5 s^4 + c_4 s^3 + c_3 s^2 + c_2 s + c_1}. \quad (16)$$

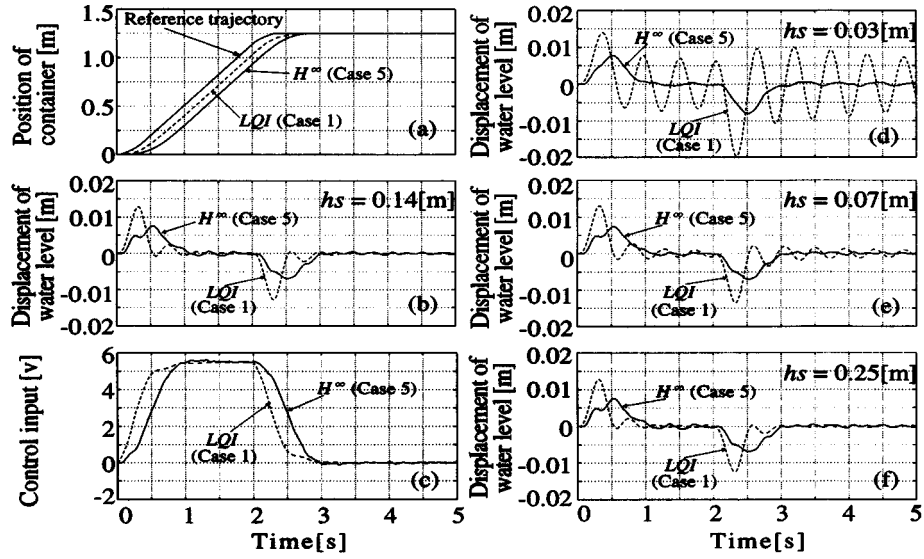


Fig. 8. Simulation results of Case1 and Case5 for the change in liquid level.

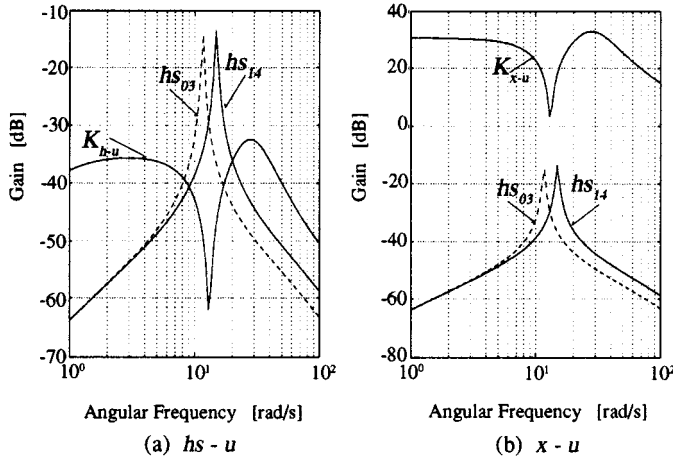


Fig. 9. Frequency responses of the controller of Case5 obtained by using the H^∞ control theory.

Fig. 9(a) shows the frequency response from the sloshing to the control input and Fig. 9(b) from the position error to the control input, and where hs_{03} and hs_{14} represent the frequency response of the model at $hs = 0.03$ [m] and 0.14 [m], respectively.

From these results, it can be seen that the gains decrease at around the resonance frequency of sloshing. Therefore, it is clear that this controller is well designed, because it does not cause excessive sloshing. It became clear that the H^∞ control system designed with the proposed nominal model suppressed sloshing, even when liquid levels are very low in the simulations, compared to the results of H^∞ control designed with the nominal liquid level $hs = 0.14$ [m].

To sum up, in order to make the system more robust than the conventional results in Case1, the selection of a suitable nominal model in Case2, the calculation of the optimum reference trajectory in Case3, and the design of the control system using robust control theory in Case4 were all necessary exercises. Thus, Case5 shows better results than any of the other cases for all performance indicators.

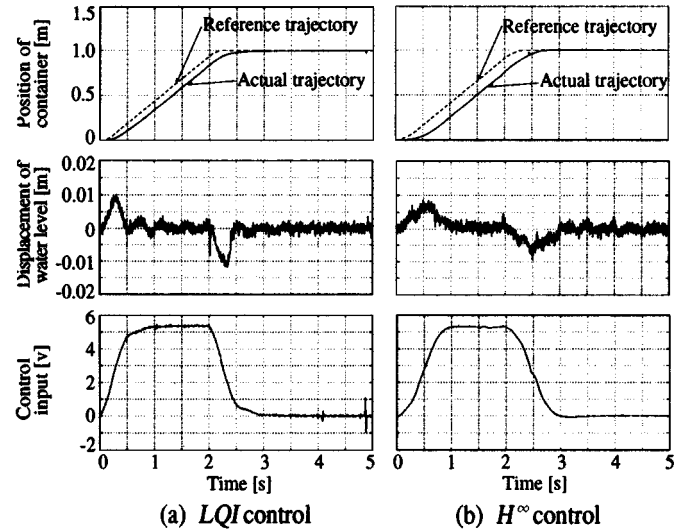


Fig. 10. Experimental results of Case1 and Case5 for liquid level $hs = 0.14$ [m].

C. Experimental Results

Experimental results for liquid level $hs = 0.14$ [m] and the changes in static liquid level are shown in Figs. 10 and 11, respectively. The experiments were carried out under the same conditions as the simulations.

Both the H^∞ control and the LQI control methods suppressed the sloshing quite well when the liquid levels were higher than 0.14 [m], as shown in Figs. 10 and 11. However, in both the experiments and in the simulation, the residual vibration of the LQI control persists as the liquid levels decrease, and therefore the H^∞ controller is superior to the LQI control system for the present problem. Also, the control input of the H^∞ control system is scarcely influenced by observational noise on the positional data.

Therefore, it became clear that the proposed method could realize a control system that could guarantee robustness to

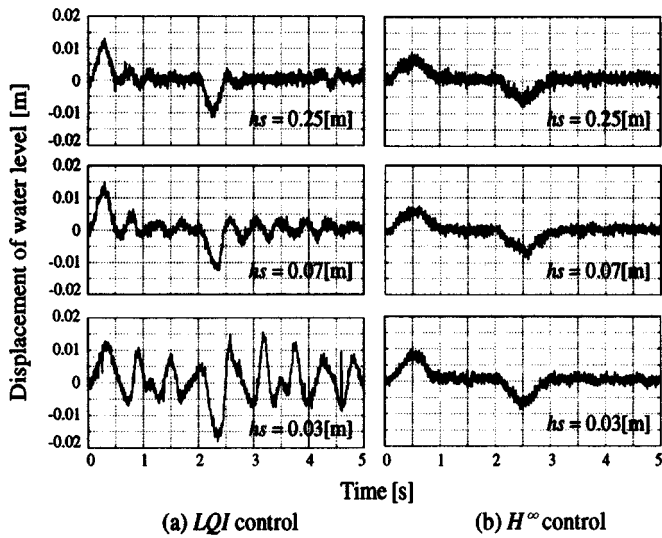


Fig. 11. Experimental results of Case 1 and Case 5 for the change in liquid level.

changes in liquid level without any deterioration of the transfer time and so on, when compared with a conventional control method [8] such as LQI control.

VII. AN ACTIVE TRANSFER SYSTEM WITH ROTATIONAL MOTION

With the control system presented in the previous sections, good control performance was obtained at the endpoints of the acceleration and deceleration phases. However, sloshing was generated during the acceleration and deceleration stages, and it is necessary to avoid sloshing throughout the entire transfer interval in order to avoid overflow and contamination of the molten metal. A complete reduction in sloshing during this phase is not possible by employing a mechanism with one-degree-of-freedom if the transfer speed is not slowed down. Hence, we have proposed a transfer machine that incorporates two degrees-of-freedom.

A. Experimental Apparatus

A schematic diagram of the experimental apparatus with one rotational motion in addition to one directional transfer action is shown in Fig. 12. This apparatus only differs from that shown in Fig. 1 in that the container is exchanged for an active container with a rotational motion capability newly installed in addition to the one directional transfer system. With respect to the rotational motion, the container is rotated by a dc servo-motor using a timing belt, and the angle of the container is detected by an encoder fitted to the rotational axis. The other instruments are the same as those described in the previous section.

B. Model with Rotary Motion

1) *Sloshing Model*: The rotational motion is added to the pendulum-type sloshing model of (17), and a new model is proposed that can be described as a sloshing model that takes into consideration rotational motion. The principles of this model are shown in Fig. 13, and by considering the moment balance

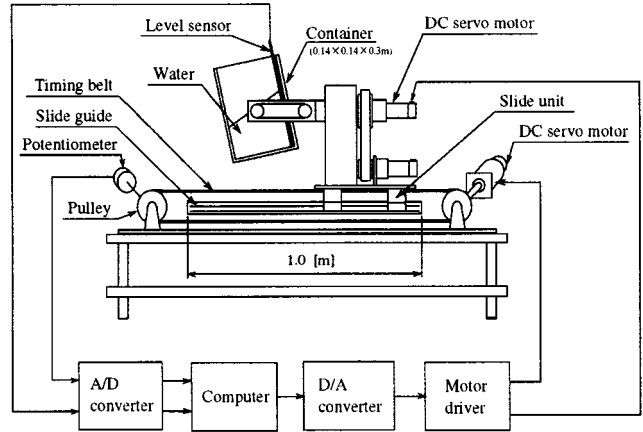


Fig. 12. Schematic diagram of experimental apparatus for active transfer with rotational motion.

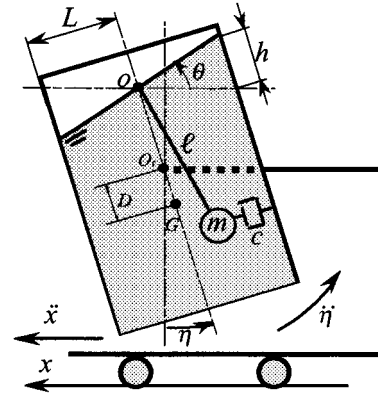


Fig. 13. Sloshing model with rotational motion.

around the fulcrum of a pendulum, the following equation is derived:

$$J \frac{d^2 \theta}{dt^2} = -c \frac{ld(\theta - \eta)}{dt} \cos^2 \theta - mgl \sin \theta + m\ddot{x} \ell \cos \theta - m\ell D \frac{d^2 \eta}{dt^2} \cos \theta \quad (17)$$

where

- J moment of inertia ($J = m\ell^2$) around the fulcrum of the pendulum O ;
- O_r center of revolution;
- D distance between the center of revolution and the center of gravity;
- θ angle of the pendulum model from horizontal level;
- η angle of the container;
- $\ddot{\eta}$ angular acceleration for container rotation;
- \ddot{x} acceleration for linear transfer applied to the container.

Linearization of (17) gives

$$\ddot{\theta} = -\frac{c}{m}(\dot{\theta} - \dot{\eta}) - \frac{g}{\ell}\theta + \frac{1}{\ell}\ddot{x} \quad (18)$$

where the force $(D/\ell)\ddot{\eta}$ added by the rotational motion of the container is neglected, because its value is very small.

2) *System Model*: The transfer function $G_r(s)$ from the input voltage $e_2(t)$ to the angular velocity $v_2(t)$ of the container

TABLE V
NOMINAL PARAMETERS OF THE ACTIVE MODEL

Parameter	Value	Unit
Length of pendulum, ℓ	0.0550	m
Coefficient of viscosity, c	0.5390	Ns/kg
Mass of liquid, m	0.9750	kg
Nominal level, hs	0.0497	m
Motor gain, K_m	0.0931	m/sV
Time constant, T_m	0.0125	s
Motor gain, K_r	-0.5507	rad/sV
Damping factor, ζ	0.3778	-
Natural angular frequency, ω_n	41.446	rad/s
Distance between O_r and G , D	0.0652	m

rotation is given by the second-order lag model shown in (19). The model parameters were obtained by adding a couple of sinusoidal-wave inputs to the apparatus

$$G_r(s) = \frac{V_2(s)}{E_2(s)} = \frac{K_r \omega_n^2}{s^2 + 2\zeta \omega_n s + \omega_n^2}. \quad (19)$$

The linear vector state-space equation is obtained in (20), where $u_1(t)$ is the control input of the linear transfer, $u_2(t)$ is the input of the rotational motion and h is the displacement of water level at the wall of the container, approximately represented by $h = L\theta$. Nominal parameters for the active sloshing model are shown in Table V. This model is also controllable and observable

$$\dot{\mathbf{x}} = \mathbf{A}\mathbf{x} + \mathbf{B}\mathbf{u}, \quad \mathbf{y} = \mathbf{C}\mathbf{x} \quad (20)$$

where

$$\mathbf{A} = \begin{bmatrix} 0 & 1 & 0 & 0 & 0 & 0 & 0 \\ -\frac{g}{\ell} & -\frac{c}{m} & 0 & \frac{c}{m} & 0 & 0 & -\frac{1}{\ell T_m} \\ 0 & 0 & 0 & 1 & 0 & 0 & 0 \\ 0 & 0 & 0 & 0 & 1 & 0 & 0 \\ 0 & 0 & 0 & -\omega_n^2 & -2\zeta\omega_n & 0 & 0 \\ 0 & 0 & 0 & 0 & 0 & 0 & 1 \\ 0 & 0 & 0 & 0 & 0 & 0 & -\frac{1}{T_m} \end{bmatrix}$$

$$\mathbf{B} = \begin{bmatrix} 0 & \frac{K_m}{\ell T_m} & 0 & 0 & 0 & 0 & \frac{K_m}{T_m} \\ 0 & 0 & 0 & 0 & K_r \omega_n^2 & 0 & 0 \end{bmatrix}^T$$

$$\mathbf{C} = \begin{bmatrix} L & 0 & -L & 0 & 0 & 0 & 0 \\ 0 & 0 & 0 & 0 & 0 & 1 & 0 \end{bmatrix}$$

$$\mathbf{x} = [\theta \quad \dot{\theta} \quad \eta \quad \dot{\eta} \quad \ddot{\eta} \quad x \quad \dot{x}]^T$$

$$\mathbf{y} = [h \quad x]^T, \quad \mathbf{u} = [u_1 \quad u_2]^T. \quad (21)$$

C. Robust Controller Design

An H^∞ controller with two control inputs was applied to the design of the transfer container such that the free surface of the liquid could be kept parallel to the bottom plate of the container, thus keeping the difference between the angle of the pendulum and the angle of the container at zero throughout the transfer interval. This system was also designed to enhance the robustness for this model uncertainties against the changes in liquid level, spillover avoidance and noise rejection, by the same methods as used in Section VI. The liquid level is also assumed

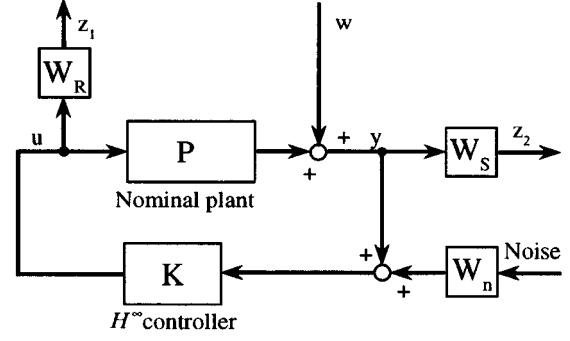


Fig. 14. Augmented closed-loop system for H^∞ control design of an active transfer.

to change over the range from 0.03 [m] to 0.25 [m]. An augmented closed-loop system is constructed as shown in Fig. 14. These specifications are represented in the following equation:

$$\left\| \begin{bmatrix} W_R R \\ W_N T \\ W_S S \end{bmatrix} \right\|_\infty < \gamma. \quad (22)$$

The uncertainty weight W_R is given to guarantee robustness for parameter uncertainty, and its value is shown in (23)

$$W_R = \begin{bmatrix} \frac{8.4 \times 10^{-2} (5s+1)(10s+1)}{(s+40)(s+70)} & \frac{2.52 \times (s+10)}{(s+70)(s+200)} \\ 0 & 0 \end{bmatrix}. \quad (23)$$

Next, a sensitivity weight W_S is given to achieve the same transfer time as the outcome of Case5 in the previous section

$$W_S = \begin{bmatrix} \frac{15000}{s+1} & 0 \\ 0 & \frac{40}{s+10^{-4}} \end{bmatrix}. \quad (24)$$

In addition to these weighting functions, W_N is given to negate the effects of stationary noise, as shown in (25), based on actual noise characteristics of measurement of both h and x

$$W_N = \begin{bmatrix} \frac{6000(2s+1)^2}{(s+100)^2} & 0 \\ 0 & \frac{10s+125}{s+125} \end{bmatrix}. \quad (25)$$

As a result of synthesis, a 16th-order controller is obtained, as described in (26), where the optimal value of γ is 1.0667×10^4

$$K(s) = \begin{bmatrix} K_{h-u1}(s) & K_{h-u2}(s) \\ K_{x-u1}(s) & K_{x-u2}(s) \end{bmatrix} \quad (26)$$

where

$$\begin{bmatrix} u_1 \\ u_2 \end{bmatrix} = \begin{bmatrix} K_{h-u1}(s) & K_{h-u2}(s) \\ K_{x-u1}(s) & K_{x-u2}(s) \end{bmatrix} \begin{bmatrix} h \\ x \end{bmatrix}. \quad (27)$$

The frequency response of the controller is shown in Fig. 15. From these results, the gains from both the position x of the container and the displacement h of the water levels to the control input u_1 are locally low at approximately the resonance frequency of sloshing. Therefore, the controller for u_1 is of the notch-filter type, one that does not oscillate the sloshing while the transfer is being carried out. On the other hand, the gain from position x of the container to the control input u_2 for the rotation is locally high at approximately the resonance frequency of sloshing. Therefore, in this system, the container is actively rotated to suppress sloshing.

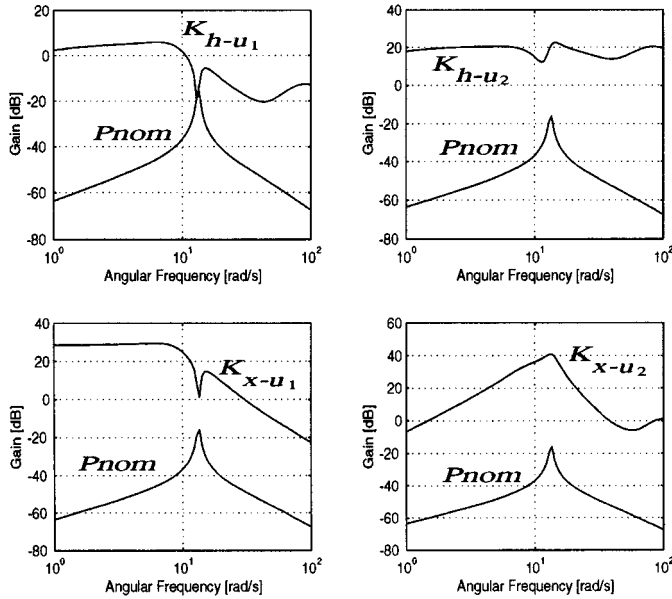


Fig. 15. Frequency responses of the controller for an active transfer.

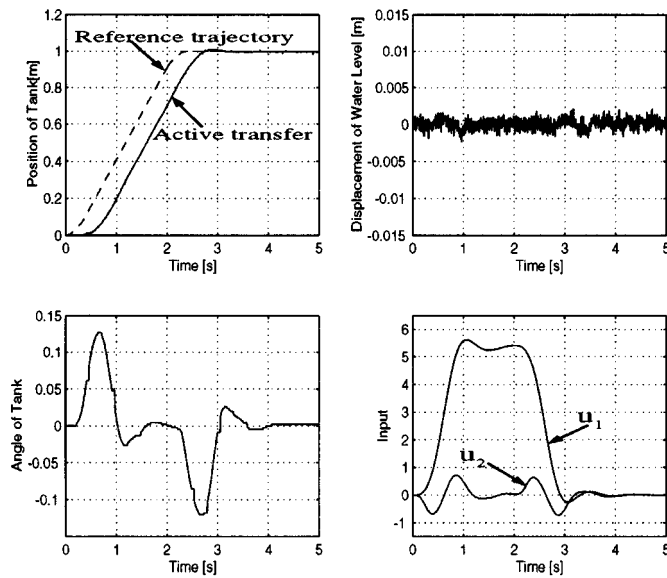


Fig. 16. Experimental results ($hs = 0.03$ [m]).

D. Control Results

In the experiments, the 1 [m]-transfer-time of this active transfer is intended to be the same as that of the normal transfer in Case5. Almost complete suppression of sloshing was realized for all transfer intervals, i.e., during acceleration, at constant velocity, during deceleration and finally after arrival, as seen in Fig. 16.

VIII. CONCLUSION

This paper presents two major points. The first is to demonstrate a robust control design by applying H^∞ control theory to a liquid container transfer with changes in static liquid level. The second is to create an active control design for liquid con-

tainer transfer by adding rotational motion to the container. The following main results have been obtained.

- The effect of changes in static liquid level at rest on the liquid container transfer system was clarified.
- A control system that effectively suppresses sloshing was designed by introducing a nominal model aimed at the middle value of the natural frequency of sloshing.
- The optimization method of Fletcher and Reeves combined with a clipping-off technique was applied to determine a reasonable reference transfer trajectory by considering the suppression of the liquid residual vibration.
- The effectiveness of the proposed H^∞ control system for model uncertainties against changes in liquid levels, spillover and both static and unpredictable noise was demonstrated by comparing with a conventional control method for the liquid container transfer system.
- Complete suppression of sloshing during the acceleration and deceleration phases of the transfer was achieved in addition to a reduction in endpoint residual vibrations by adding active rotational motion to the container.

REFERENCES

- [1] G. W. Housner, "The Dynamic Behavior of Water Tanks," *Bulletin of Seismological Society of America*, vol. 53, no. 2, pp. 381–387, 1963.
- [2] H. N. Abramson, W. H. Chu, and D. D. Kana, "Some Studies of Non-linear Lateral Sloshing in Rigid Containers," *J. Appl. Mechanics, Trans. ASME*, pp. 777–784, 1966.
- [3] R. Barron and S. W. R. Chng, "Dynamic Analysis and Measurement of Sloshing of Fluid in Containers," *J. Dyn. Syst., Measurement, Contr., Trans. ASME*, vol. 111, pp. 83–90, 1989.
- [4] R. Jeyakumaran and P. Mciver, "Approximations to Sloshing Frequencies for Rectangular Tanks with Internal Structures," *J. Eng. Math.*, vol. 29, pp. 537–556, 1995.
- [5] V. Armenio and M. L. Rocca, "On the Analysis of Sloshing of Water in Rectangular Containers: Numerical Study and Experimental Validation," *Ocean Eng.*, vol. 23, no. 8, pp. 705–739, 1996.
- [6] T. Ikeda and N. Nakagawa, "Non-Linear Vibrations of a Structure Caused by Water Sloshing in a Rectangular Tank," *J. Sound Vibration*, vol. 201, no. 1, pp. 23–41, 1997.
- [7] K. Terashima, M. Hamaguchi, and G. Schmidt, "Sloshing Analysis and Transportation Control of Rectangular Liquid Tank," in *Proc. ASCC '94*, p. 773.
- [8] M. Hamaguchi, K. Terashima, and H. Nomura, "Optimal Control of Liquid Container Transfer for Several Performance Specifications," *J. Advanced Automat. Technol.*, vol. 6, no. 6, pp. 353–360, 1994.
- [9] M. Hamaguchi, H. Motegi, K. Terashima, and H. Nomura, "Optimal Control of Transferring a Liquid Container with Boundary Element Analysis" (in Japanese), *Trans. SICE*, vol. 31, no. 9, pp. 1442–1451, 1995.
- [10] K. Terashima, G. Schmidt, and H. Nomura, "Transportation Control of Container Considering Suppression of Liquid Vibration," in *Proc. ECC '93*, 1993, p. 1297.
- [11] T. Sugie and T. Ashitani, "Optimal Transfer Control of Liquid Containers Based on Convex Optimization and H^∞ Control" (in Japanese), *Trans. SCI (Inst. Syst., Contr., Inform. Eng.)*, vol. 9, no. 4, pp. 172–178, 1996.
- [12] K. Terashima, M. Hamaguchi, and A. Kaneshige, "Motion Control of an Automotive Cart Based Cylindrical Container Considering Suppression of Liquid Oscillation on a Curve Track Transfer," in *Proc. IFAC Workshop Motion Contr. '95*, 1995, p. 845.
- [13] M. Hamaguchi, M. Yamamoto, and K. Terashima, "Modeling and Control of Sloshing with Swirling in a Cylindrical Container during a Curved Path Transfer," in *Proc. ASCC '97*, 1997, p. 233.
- [14] H. Yamagata and S. Kaneko, "Sloshing Suppression Control of Contained Liquid in a Moving Cylindrical Container" (in Japanese), *Trans. JSME*, vol. 64, no. 621, C, pp. 200–208, 1998.
- [15] M. Hamaguchi, W. Ronda, and K. Terashima, "Optimum Shape Design of Container for Liquid Transfer Considering the Damping of Sloshing," in *Proc. FLUCOME '97*, 1997, p. 639.

- [16] K. Terashima and T. Yoshida, "Nonlinear Optimal Control with Specified Frequency-range Considering Resonance Frequency and Its Application to Liquid Container Transfer," in *Proc. FLUCOME '97*, 1997, p. 767.
- [17] K. Terashima, M. Hamaguchi, and A. Kaneshige, "Optimum Control of Three-Dimensional Liquid Container Transfer and Robustness of Sloshing Suppression for the Change of Liquid Level and Viscosity" (in Japanese), *Trans. SCI*, vol. 9, no. 4, pp. 162–171, 1996.
- [18] M. Grundelius and B. Rernhardsson, "Motion Control of Open Containers with Slosh Constraints," in *Proc. 14th IFAC World Congr.*, 1999, pp. 487–492.
- [19] T. Fukuda, A. Suzuki, and H. Shibata, "Active Suppression Control of Fluid Vibration in a Container" (in Japanese), *Trans. JSME*, vol. 56, no. 532, C, pp. 99–106, 1990.
- [20] J. T. Feddema, C. R. Dohrmann, G. G. Parker, R. D. Robinett, V. J. Romero, and D. J. Schmidt, "Control for Slosh-Free Motion of an Open Container," *IEEE Contr. Syst. Mag.*, vol. 17, no. 1, pp. 29–36, 1997.
- [21] R. Fletcher and C. M. Reeves, "Function Minimization by Conjugate Gradients," *Comput. J.*, vol. 7, pp. 149–154, 1964.
- [22] V. H. Quintana and E. J. Davison, "Clipping-off Gradient Algorithms to Compute Optimal Controls with Constrained Magnitude," *Int. J. Contr.*, vol. 20, no. 2, pp. 243–255, 1974.
- [23] G. Zames and B. A. Francis, "Feedback, Minimax Sensitivity and Optimal Robustness," *IEEE Trans. Automat. Contr.*, vol. 28, pp. 585–601, 1983.
- [24] J. C. Doyle, K. Glover, P. Khargonekar, and B. A. Francis, "State-Space Solutions to Standard H^2 and H^∞ Control Problems," *IEEE Trans. Automat. Contr.*, vol. 34, pp. 831–847, 1989.



Kazuhiko Terashima (S'79–M'81) was born in Osaka, Japan, in 1952. He received the B.S. and M.S. degrees from Kyoto Institute of Technology, in 1976 and 1978, respectively, and a Ph.D. degree in mechanical engineering from Kyoto University, in 1982.

Since 1982, he has worked in Production Systems Division, Toyohashi University of Technology, Aichi, Japan, and he has been a Professor since 1994. He was a Visiting Research Fellow at Technische Universität München, München, Germany, from September 1991 to September 1992. His research interests lie in the analysis and design of control systems, and the application to motion control, robotics, and intelligent systems.



Ken'ichi Yano (S'98–A'99) was born in Osaka, Japan, in 1969. He received the B.E. and the M.E. degree in production systems engineering from Toyohashi University of Technology, Aichi, Japan, in 1994 and 1996, respectively. He received the D.E. degree in electronic and information engineering from Toyohashi University of Technology, Aichi, Japan, in 1999.

He has been with Toyohashi University of Technology since 1999 as a Research Associate. His research interests include robust control theory and

its applications to a liquid container transfer system and an automatic pouring system.